

*Supplementary Information for*

# **Hydrogen peroxide emissions from surface cleaning in a single-family residence**

Pedro A. F. Souza<sup>1</sup>, Shan Zhou<sup>2a</sup>, and Tara F. Kahan<sup>1,\*</sup>

<sup>1</sup>Department of Chemistry, University of Saskatchewan, Saskatoon, SK, Canada

<sup>2</sup> Department of Civil and Environmental Engineering, Rice University, Houston, TX, US

<sup>a</sup>Currently at Department of Earth and Atmospheric Sciences, University of Houston, Houston, TX, US

\*Corresponding Author: Tara Kahan, Department of Chemistry, University of Saskatchewan, Saskatoon, Saskatchewan S7N 5C9, Canada. Phone: (306) 966-1168 E-mail: [tara.kahan@usask.ca](mailto:tara.kahan@usask.ca)

Pages S1 – S11

Figures S1 – S7

Tables S1 – S3

## SUPPLEMENTAL METHODS

### Determination of peaks for kinetic analysis

Decay rate constants of  $\text{H}_2\text{O}_2$  ( $k$ ) were calculated using first-order exponential regression (Eq. 1) for selected  $\text{H}_2\text{O}_2$  emission profiles following cleaning events. For such analysis, we either removed the large fluctuations (i.e., sharp spikes) seen in most of the cleaning events (as illustrated in Figure S2) or selected an adequate  $C_0$  (the initial mixing ratio) to minimize the large fluctuations.

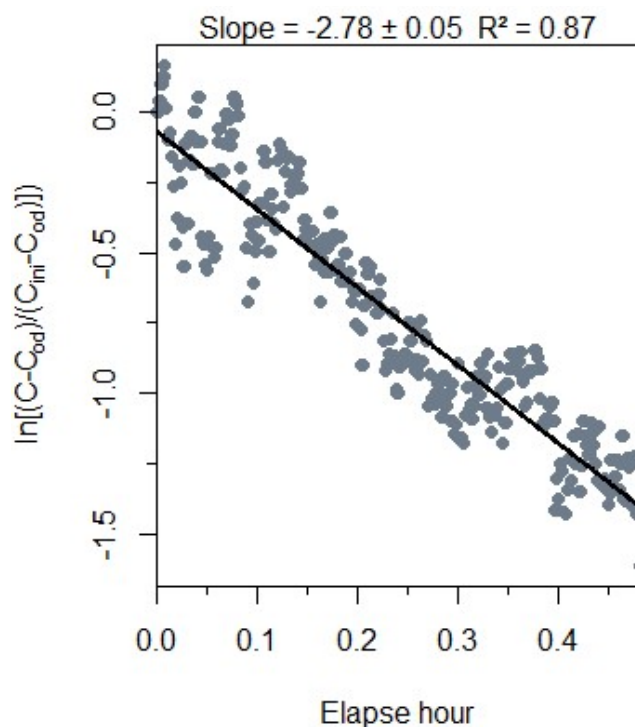


**Figure S1.** Representative log-normalized decay profile for near counter experiment during regular cleaning. Slope represents the decay rate constant ( $k$ ).

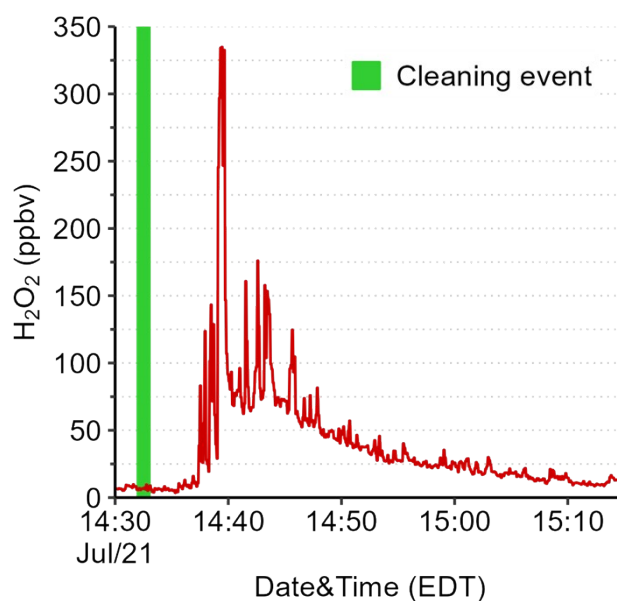


**Figure S2.** Temporal profile of  $H_2O_2$  mixing ratios observed in the house for a regular cleaning of dining room table when doors/windows were closed.

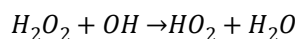
### OH steady-state concentration ( $[OH]_{ss}$ )

Predicted  $[OH]_{ss}$  was calculated using the simplified steady-state approximation described by Zhou et al.:<sup>1</sup>

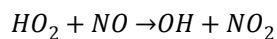
$$[OH]_{ss} = \frac{J_{HONO}[HONO] + 2J_{H_2O_2}[H_2O_2]}{k_{OH+NO}[NO] + k_{OH+NO_2}[NO_2] + k_{OH+HONO}[HONO]} \quad [S1]$$

where  $J_{HONO}$  and  $J_{H_2O_2}$  are the photolysis rate constants ( $s^{-1}$ ) of nitrous acid and hydrogen peroxide, respectively;  $k_{OH+NO}$ ,  $k_{OH+NO_2}$ ,  $k_{OH+HONO}$ , and  $k_{OH+H_2O_2}$  are the rate constants ( $cm^3 \text{ molec}^{-1} s^{-1}$ ) for the reactions between OH and NO, OH and  $NO_2$ , OH and HONO, and OH and  $H_2O_2$ , respectively; and  $[X]$  represents the concentration of gas-phase species ( $\text{molecule cm}^{-3}$ ), with  $X = HONO, H_2O_2, NO, \text{ or } NO_2$ .

Hydrogen peroxide can be a sink for OH (R1). We do not expect reaction with  $H_2O_2$  to contribute greatly to OH loss, as  $HO_2$  reacts quickly with NO to form OH (R2). Nitric oxide concentrations in residences are on the order of  $1 \times 10^{11} \text{ molecule cm}^{-3}$  (4 ppbv) in the absence of combustion (e.g., use of gas stoves).<sup>2</sup> At these NO concentrations we can assume that  $HO_2$  is rapidly converted to OH, and loss of OH to reaction with  $H_2O_2$  can be rejected. This assumption is also made for loss of OH to reaction with volatile organic compounds (VOCs), which also results in the formation of  $HO_2$ . However, we also calculated  $[OH]_{ss}$  with loss to reaction with  $H_2O_2$  included to provide a lower limit for  $[OH]_{ss}$  (S2).



[R1]



[R2]

$$[OH]_{SS} = \frac{J_{HONO}[HONO] + 2J_{H_2O_2}[H_2O_2]}{k_{OH+NO}[NO] + k_{OH+NO_2}[NO_2] + k_{OH+HONO}[HONO] + k_{OH+H_2O_2}[H_2O_2]} \quad [S2]$$

Table S3 shows kinetic parameters used for  $[OH]_{ss}$  calculations. Table S4 shows predicted  $[OH]_{ss}$  with and without  $H_2O_2$  included as a sink at the  $H_2O_2$  concentrations shown in Table 3. When loss to  $H_2O_2$  was not considered,  $[OH]_{ss}$  was predicted to increase by up to 21% compared to pre-cleaning levels (i.e., with HONO photolysis as the sole OH source), but including it led to a predicted reduction in  $[OH]_{ss}$  of 91%.

**Table S1.** Values used for determining  $[OH]_{ss}$  in Eq. S1. Photolysis rate constants ( $J$ ) are from Kowal et al.<sup>3</sup>, and the rate constants ( $k_{OH+X}$ ) are from Burkholder et al.<sup>4</sup>

Gas-phase species	$J$ ( $s^{-1}$ )	$k_{OH+X}$ ( $cm^3 \text{ molec}^{-1} s^{-1}$ )	$[X]$ ( $\text{molec cm}^{-3}$ )
$H_2O_2$	$1.4 \times 10^{-7}$	$1.8 \times 10^{-12}$	Varies <sup>a</sup>
<b>HONO</b>	$2.2 \times 10^{-4}$	$6.9 \times 10^{-12}$	$1.2 \times 10^{11}$
<b>NO</b>	-	$7.4 \times 10^{-12}$	$1.0 \times 10^{11}$
<b>NO<sub>2</sub></b>	-	$1.3 \times 10^{-11}$	$1.0 \times 10^{11}$

a) Presented on Table 3 and Table S4 with units of ppbv

**Table S2.** Predicted  $[OH]_{ss}$  following cleaning in sunlit air volumes using steady-state calculations Eq. S1 ( $H_2O_2$  not considered a sink) and S2 ( $H_2O_2$  considered a sink).

$[H_2O_2]$ (ppb)	$[OH]_{ss}$ from Eq. S1 ( $10^6$ molecule $cm^{-3}$ )	$[OH]_{ss}$ from Eq. S2 ( $10^6$ molecule $cm^{-3}$ )
1	9.4	9.3
135	9.7	3.1
323	10.2	1.7
840	11.4	0.8

While ignoring  $H_2O_2$  as an OH sink may be overly simplistic, the small increases in  $[OH]_{ss}$  using this approach (i.e., Eq. S1) are in good agreement with those from Zhou et al.<sup>5</sup> In that work,  $[OH]_{ss}$  was predicted using an indoor atmospheric chemistry box model.<sup>5</sup> The model used was based on the master chemical model (MCM) and included explicit chemical reactions for ~5000 distinct species. Loss of OH to reaction with  $H_2O_2$  and VOCs was included in the steady-state calculations, as was regeneration of OH from  $HO_2$  via R2.<sup>6</sup> In that work, the model predicted peak  $[OH]_{ss}$  to increase by ~10% when measured  $H_2O_2$  concentrations increased to ~313 ppbv following cleaning.<sup>5</sup> Using Eq. S1, we predict  $[OH]_{ss}$  to increase by ~8% at that  $H_2O_2$  concentration. Conversely, using Eq. S2 results in a predicted *decrease* of  $[OH]_{ss}$  of ~81%. The agreement with  $[OH]_{ss}$  predicted by the box model obtained by Eq. S1 gives us confidence that this simplified steady-state equation is appropriate for  $[OH]_{ss}$  calculation under the conditions of this study, and that R1 should not be included as a loss term for OH. We note that this approach is valid when NO levels are high. When NO levels are low (due, for example, to titration by  $O_3$ ),  $HO_2$  will not be completely converted to OH, and R1 might become a permanent sink. For example, we used the box model described above to calculate radical concentrations in a hospital room during the use of common gas-phase disinfectants including  $H_2O_2$ .<sup>7</sup> At high  $H_2O_2$  concentrations (up to 500 ppmv is used during disinfection),  $[OH]_{ss}$  was predicted to be only ~30% of that in the absence of added  $H_2O_2$ , despite very large OH formation rates (on the order of  $10^9$  molecule  $cm^{-3}$   $s^{-1}$ ). This decrease was attributed to OH loss via R1. Once  $H_2O_2$  levels in the room decayed to 1 ppmv, we predicted  $[OH]_{ss}$  to have increased to 70% of initial levels. We note that predicted NO concentrations in the hospital room were <150 pptv; regeneration of OH from  $HO_2$  via R2 will be much slower than in residences, where NO concentrations are often more than 20× higher.

ADDITIONAL SUPPLEMENTAL FIGURES

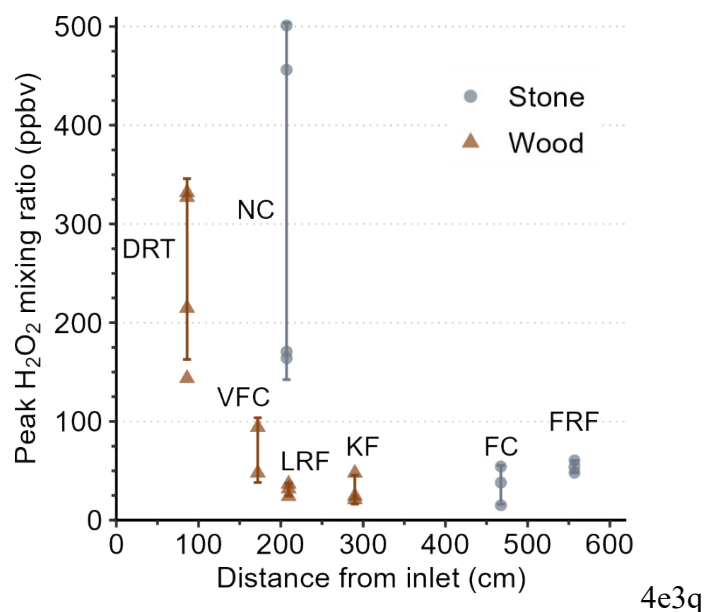


**Figure S3.** Peak  $H_2O_2$  levels as a function of average distance from inlet for controlled regular cleaning events. Abbreviated texts indicate surface types listed in Table 1. Error bars represent the standard deviation.

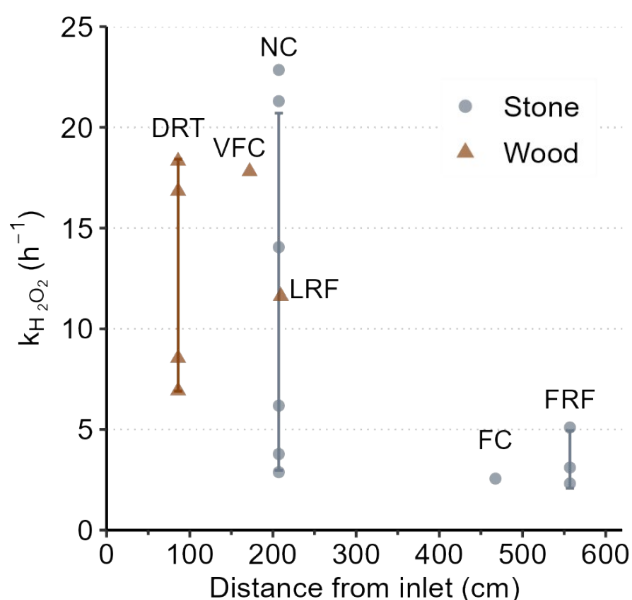


**Figure S4.**  $H_2O_2$  decay rate constants as a function of average distance from inlet for controlled regular cleaning events. Abbreviated texts indicate surface types listed in Table 1. Error bars represent the standard deviation.

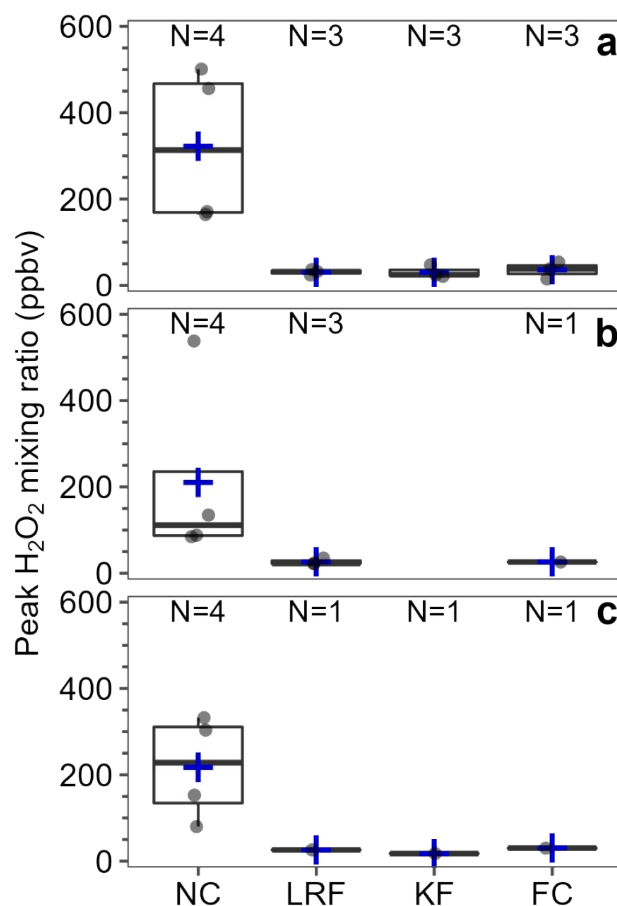


**Figure S5.** Statistics of peak H<sub>2</sub>O<sub>2</sub> levels for regular cleaning of four surfaces under different conditions: **(a)** full area cleaned with closed doors/windows, **(b)** half area cleaned with closed doors/windows, and **(c)** full area cleaned with patio doors open. The box and whisker plots show the median (line), mean (blue marker), first and third quartiles (box), and minima and maxima (whiskers). The number over each box and whisker plot indicates the number of cleaning events for that condition.

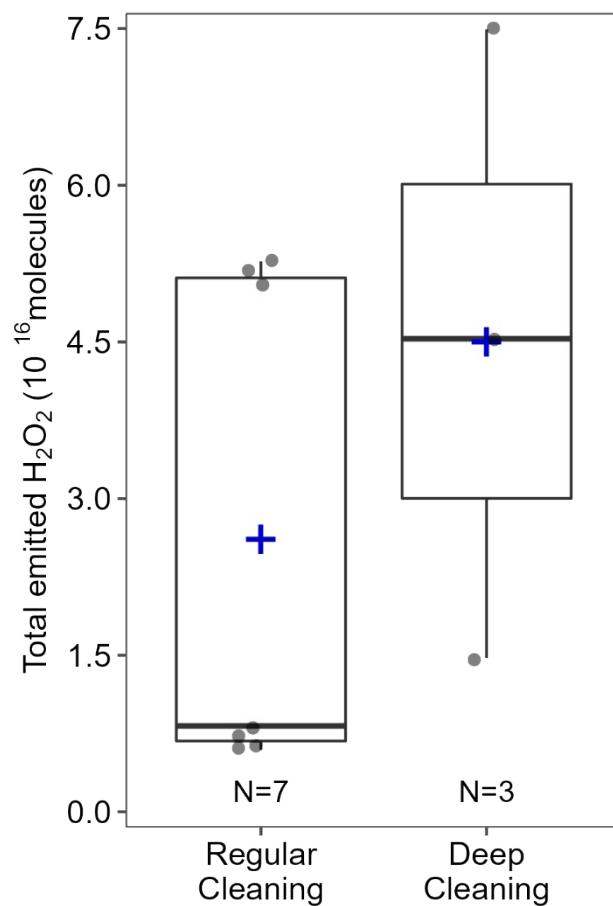


**Figure S6.** Statistics of total emitted H<sub>2</sub>O<sub>2</sub> molecules for regular and deep cleaning of the near counter and living room floor. The box and whisker plots show the median (line), mean (blue marker), first and third quartiles (box), and minimum and maximum (whiskers). The number under each box and whisker plot indicates the number of cleaning events for that condition.



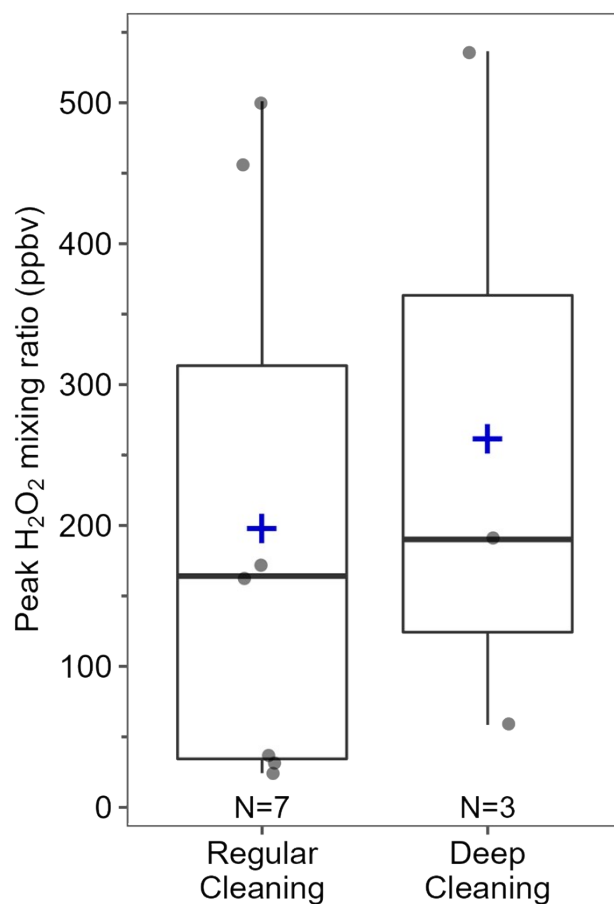


**Figure S7.** Statistics of peak H<sub>2</sub>O<sub>2</sub> levels for regular and deep cleaning of the near counter and living room floor. The box and whisker plots show the median (line), mean (blue marker), first and third quartiles (box), and minimum and maximum (whiskers). The number under each box and whisker plot indicates the number of cleaning events for that condition.

## ADDITIONAL SUPPLEMENTAL TABLES

**Table S3.** Mean peak and total H<sub>2</sub>O<sub>2</sub> mixing ratios and mean decay rate constants ( $k_{H_2O_2}$ ) for cleaning events when full and half area were cleaned.

Surface	Full area cleaned				Half area cleaned			
	Peak H <sub>2</sub> O <sub>2</sub> (ppbv)	Total H <sub>2</sub> O <sub>2</sub> (10 <sup>15</sup> molecules)	$k_{H_2O_2}$ (h <sup>-1</sup> )	N	Peak H <sub>2</sub> O <sub>2</sub> (ppbv)	Total H <sub>2</sub> O <sub>2</sub> (10 <sup>15</sup> molecules)	$k_{H_2O_2}$ (h <sup>-1</sup> )	N
NC	323 ± 181	40.5 ± 22.3	11.8 ± 8.9	4	211 ± 219	21.5 ± 17.1	14.7 ± 8.3	4
LRF	31.0 ± 6.4	6.86 ± 1.21	11.6	3	27.0 ± 7.5	4.53 ± 1.39	-	3
KF	31.0 ± 14.5	8.86 ± 4.40	-	3	-	-	-	0
FC	35.8 ± 19.7	10.8 ± 8.4	2.56	3	26.2	7.58	-	1

**Table S4.** Mean peak mixing ratios, total H<sub>2</sub>O<sub>2</sub> molecules emitted, and mean decay rate

Surface	Closed doors/windows				Opened doors/windows			
	Peak H <sub>2</sub> O <sub>2</sub> (ppbv)	Total H <sub>2</sub> O <sub>2</sub> (×10 <sup>15</sup> molecules)	$k_{H_2O_2}$ (h <sup>-1</sup> )	N	Peak H <sub>2</sub> O <sub>2</sub> (ppbv)	Total H <sub>2</sub> O <sub>2</sub> (×10 <sup>15</sup> molecules)	$k_{H_2O_2}$ (h <sup>-1</sup> )	N
NC	323 ± 181	40.5 ± 22.3	11.8 ± 8.9	4	217 ± 121	31.8 ± 14.6	27.4 ± 22.8	4
LRF	31.0 ± 6.4	6.86 ± 1.21	11.6	3	26.2	4.05	-	1
KF	31.0 ± 14.5	8.86 ± 4.40	-	3	17.8	6.76	-	1
FC	35.8 ± 19.7	10.8 ± 8.4	2.56	3	30.3	6.56	4.9	1

constants ( $k_{H_2O_2}$ ) for cleaning events when doors/windows were closed and opened.

## REFERENCES

- (1) Zhou, S.; Kahan, T. F. Spatiotemporal Characterization of Irradiance and Photolysis Rate Constants of Indoor Gas-Phase Species in the UTest House during HOMEChem. *Indoor Air* **2022**, *32* (1), e12964. <https://doi.org/10.1111/ina.12966>.
- (2) Zhou, S.; Young, C. J.; VandenBoer, T. C.; Kowal, S. F.; Kahan, T. F. Time-Resolved Measurements of Nitric Oxide, Nitrogen Dioxide, and Nitrous Acid in an Occupied New York Home. *Environ. Sci. Technol.* **2018**, *52* (15), 8355–8364. <https://doi.org/10.1021/acs.est.8b01792>.
- (3) Kowal, S. F.; Allen, S. R.; Kahan, T. F. Wavelength-Resolved Photon Fluxes of Indoor Light Sources: Implications for HO<sub>x</sub> Production. *Environ. Sci. Technol.* **2017**, *51* (18), 10423–10430. <https://doi.org/10.1021/acs.est.7b02015>.
- (4) Burkholder, J. B.; Sander, S. P.; Abbatt, J. P. D.; Barker, J. R.; Cappa, C.; Crouse, J. D.; Dibble, T. S.; Huie, R. E.; Kolb, C. E.; Kurylo, M. J.; Orkin, V. L.; Percival, C. J.; Wilmouth, D. M.; Wine, P. H. *Chemical Kinetics and Photochemical Data for Use in Atmospheric Studies, Evaluation No. 19*; JPL Publication 19-5; California Institute of Technology: Jet Propulsion Laboratory, Pasadena, 2019. <https://jpldataeval.jpl.nasa.gov/>.
- (5) Zhou, S.; Liu, Z.; Wang, Z.; Young, C. J.; VandenBoer, T. C.; Guo, B. B.; Zhang, J.; Carslaw, N.; Kahan, T. F. Hydrogen Peroxide Emission and Fate Indoors during Non-Bleach Cleaning: A Chamber and Modeling Study. *Environ. Sci. Technol.* **2020**, *54* (24), 15643–15651. <https://doi.org/10.1021/acs.est.0c04702>.
- (6) Carslaw, N. A New Detailed Chemical Model for Indoor Air Pollution. *Atmos. Environ.* **2007**, *41* (6), 1164–1179. <https://doi.org/10.1016/j.atmosenv.2006.09.038>.
- (7) Wang, Z.; Kowal, S. F.; Carslaw, N.; Kahan, T. F. Photolysis-Driven Indoor Air Chemistry Following Cleaning of Hospital Wards. *Indoor Air* **2020**, *30* (6), 1241–1255. <https://doi.org/10.1111/ina.12702>.